Eur Respir J 2011; 38: 1444–1452
DOI: 10.1183/09031936.00129610

IκBα glutathionylation and reduced histone H3 phosphorylation inhibit eotaxin and RANTES

P. Seidel*, M. Roth#, Q. Ge¶, I. Merfort+, C.T. S'ng# and A.J. Ammit*

ABSTRACT: Airway smooth muscle cells (ASMCs) secrete eotaxin and RANTES (regulated on activation, normal T-cell expressed and secreted) in response to tumour necrosis factor (TNF)-α, which is inhibited by the nuclear factor (NF)-κB inhibitor dimethylfumarate (DMF). NF-κB/IκB (inhibitor of NF-κB) glutathionylation and changes in chromatin remodelling can inhibit NF-κB activity. In this study, we determined whether NF-κB/IκB glutathionylation and reduced histone H3 phosphorylation might underlie the inhibitory effect of DMF on NF-κB activity, and eotaxin and RANTES secretion.

Primary human ASMCs were treated with DMF, diamide and/or glutathione (GSH) ethylester (OEt) prior to TNF-α stimulation and were subsequently analysed by ELISA, electrophoretic mobility shift assay, immunofluorescence, co-immunoprecipitation or immunoblotting.

DMF reduced intracellular GSH and induced IκBα glutathionylation (IκBα-SSG), which inhibited IκBα degradation, NF-κB p65 nuclear entry and NF-κB/DNA binding. In addition, DMF inhibited the phosphorylation of histone H3, which was possibly mediated by the inhibitory effect of DMF on mitogen- and stress-activated protein kinase (MSK)-1. However, p38 mitogen-activated protein kinase (MAPK), extracellular signal-regulated kinase MAPK and MAPK phosphatase-1, upstream of MSK-1, were not inhibited by DMF. Importantly, DMF-mediated effects on NF-κB, histone H3, eotaxin and RANTES were reversed by addition of GSH-OEt.

Our data suggest that DMF inhibits NF-κB-dependent eotaxin and RANTES secretion by reduction of GSH with subsequent induction of IκBα-SSG and inhibition of histone H3 phosphorylation. Our findings offer new potential drug targets to reduce airway inflammation in asthma.

KEYWORDS: Asthma, glutathionylation, histone H3, IκBα, mitogen- and stress-activated protein kinase-1

Asthma is a chronic inflammatory disease of the airways. The airways of asthmatic patients are characterised by an increased number of eosinophils and increased sputum eosinophil counts correlated with asthma severity [1]. The chemokines eotaxin and RANTES (regulated on activation, normal T-cell expressed and secreted) are centrally involved in the recruitment of eosinophils into the inflamed airway tissue and both chemokines are elevated in bronchial biopsies of asthmatic donors [2].

Both chemokines have been detected in airway smooth muscle *in vivo* [3, 4] and tumour necrosis factor (TNF)-α increased human airway responsiveness [5]. In asthma, local cytokine secretion may cause eosinophil infiltration along a gradient into the submucosa [6]. In cultured human airway smooth muscle cells (ASMCs), TNF-α activates the transcription factor nuclear factor (NF)-κB and induces the expression of cytokines [7]. *In vitro* studies have shown that TNF-α-induced eotaxin and RANTES secretion by ASMCs is downregulated by inhibition of NF-κB [7, 8].

NF-κB forms dimers consisting of the subunits p50, p52, p65 (RelA), RelB and c-Rel. In unstimulated cells, NF-κB is retained in the cytosol in a complex formed with IκB (inhibitor of NF-κB) proteins. Cell stimulation induces degradation of IκB, leaving free, active NF-κB to migrate into the nucleus, where it binds DNA to initiate gene transcription [9].

The IκB protein IκBα contains cysteine thiols, which are susceptible to redox-regulated post-translational modifications [10]. One such reversible modification is protein glutathionylation (protein-SSG), whereby a cysteine-thiol of a protein (protein-SH), forms a disulfide bond with the cysteine-thiol of glutathione (GSH). Protein-SSG is inducible by reduction of the

AFFILIATIONS
*Respiratory Research Group, Faculty of Pharmacy,
¶Woolcock Institute of Medical Research, University of Sydney, Sydney, Australia.
#Pulmonary Cell Research, Division of Research and Pneumology, Dept of Internal Medicine, University Hospital Basel, Basel, Switzerland.
+Institute of Pharmaceutical Sciences, Dept of Pharmaceutical Biology and Biotechnology, University of Freiburg, Freiburg, Germany.

CORRESPONDENCE
M. Roth
Pneumology
University Hospital Basel
Petersgraben 4
CH-4031 Basel
Switzerland
E-mail: rothmic@uhbs.ch

Received:
Aug 12 2010
Accepted after revision:
June 14 2011
First published online:
June 30 2011

European Respiratory Journal
Print ISSN 0903-1936
Online ISSN 1399-3003

intracellular GSH level [11] and has been shown to result in an inhibition of NF-κB nuclear entry and binding to DNA [12, 13]. Dimethylfumarate (DMF) reduces cellular glutathione in many different cell types [14–16], and has also been shown to inhibit the nuclear entry of NF-κB and subsequent binding to DNA in ASMCs [7]. Therefore, IκBα-SSG is a possible mechanism by which DMF inhibits NF-κB activity.

Histone H3 phosphorylation is crucial for chromatin relaxation and optimal binding of transcription factors to their corresponding DNA sequences [17]. Histone H3 phosphorylation at Ser10 occurs in the promoters of NF-κB-regulated cytokines, such as RANTES [18], and has been shown to increase the accessibility of NF-κB binding sides [19]. Mitogen- and stress-activated protein kinase (MSK)-1 phosphorylates histone H3 at Ser10 [20], and MSK-1 is inhibited by DMF in ASMCs and keratinocytes [7, 21]. Therefore, inhibition of MSK-1-mediated histone H3 phosphorylation by DMF may contribute to its inhibitory effect on NF-κB-dependent chemokine secretion.

In this study in human ASMCs, we aimed to determine whether glutathionylation of NF-κB/IκBα and reduced histone H3 phosphorylation underlie the inhibitory effect of DMF on NF-κB-dependent eotaxin and RANTES secretion.

MATERIAL AND METHODS

Material

All chemicals were purchased from Sigma (St Louis, MO, USA) unless otherwise specified.

Isolation and culture of human ASMCs

Human ASMCs were isolated from the bronchi of patients undergoing surgical resection for carcinoma or lung transplantation, after written informed consent was obtained, as approved by the South West Sydney Area Health Service and the Human Ethics Committee, University of Sydney (Sydney, Australia) and by the local ethics committee of the University Hospital Basel (Basel, Switzerland). Primary ASMC lines were isolated and characterised as previously described [7, 22]. ASMCs were used between passages 5 and 8, and experiments were performed in ASMCs of at least three different donors; the demographic data of the patients are summarised in table 1.

Intracellular GSH level

Confluent ASMCs were deprived of serum (24 h) and were then treated with DMF (50 μM) or the drug vehicle dimethylsulfoxide (DMSO; 0.05%) for 1 or 3 h. The GSH assay was performed according to the manufacturers' protocol (Glutathione Assay Kit; BioVision, San Diego, CA, USA).

IκBα-SSG

Confluent ASMCs were deprived of serum (24 h) and incubated with diamide (100–500 μM for 30 min), or with DMF (50 μM for 1 h) and/or GSH ethylester (OEt) (1 mM for 90 min) before TNF-α stimulation (10 ng·mL^{-1} for 30 min; R&D Systems, Minneapolis, MN, USA). The Catch and Release version 2.0 Reversible Immunoprecipitation System (Millipore, Billerica, MA, USA) was used to perform co-immunoprecipitation (IP) of the NF-κB/IκB complex. Briefly, ASMCs were lysed (50 mM

TABLE 1 Demographic data of the patients

Patient	Sex	Age yrs	Diagnosis	Smoker	FEV_1 L (% pred)		FVC L (% pred)	
					L	% pred	L	% pred
1	Male	49	Emphysema	NA	N/A	N/A	N/A	N/A
2	Female	64	Emphysema	NA	N/A	N/A	N/A	N/A
3	Male	62	Mass	Smoker		88		96
4	Male	69	Nonsmall cell carcinoma	Ex-smoker	N/A	N/A	N/A	N/A
5	Male	26	Bronchiolitis obliterans	NA	N/A	N/A	N/A	N/A
6	Male	76	Small cell carcinoma, COPD	Ex-smoker	1.4		1.85	
7	Female	59	NSCLC	Ex-smoker	2.93	82	3.43	
8	Female	66	Carcinoma	Ex-smoker	N/A	N/A	N/A	N/A
9	Male	65	NSCLC	Smoker	3.11	76	3.98	3.98
10	Male	41	Emphysema	NA	N/A	N/A	N/A	N/A
11	Male	59	Emphysema	NA	N/A	N/A	N/A	N/A
12	Male	66	NSCLC	Smoker	3.4	72	4.8	
13	Male	70	NSCLC	NA	N/A	N/A	N/A	N/A
14	Female	45	Donor	NA	N/A	N/A	N/A	N/A
15	Male	64	Carcinoma	Ex-smoker	3.2		3.9	
16	Male	70	Carcinoma	Ex-smoker	2.14		3.84	
17	Female	51	NSCLC	smoker	3.11	81	3.46	
18	Male	62	NSCLC	Ex-smoker	1.98	70	2.37	
19	Male	67	COPD	Ex-smoker	0.93	78	1.29	
20	Female	47	NSCLC	Ex-smoker	2.75	65	2.96	

None of the patients had received any therapy before lung tissue sampling. FEV_1: forced expiratory volume in 1 s; % pred: % predicted; FVC: forced vital capacity; COPD: chronic obstructive pulmonary disease; NSCLC: nonsmall-cell lung carcinoma; N/A: not available.

Tris-HCl, pH 7.5; 120 mM NaCl; 1% NP-40; 1× protease inhibitor cocktail) and the samples were incubated with antibodies against NF-κB p65 (4 μg; C-20) or NF-κB p50 (4 μg; H-119), or the normal rabbit immunoglobulin (Ig)G negative control (4 μg; all Santa Cruz Biotechnology, Santa Cruz, CA, USA) in spin columns containing 0.5 mL IP capture resin. IP eluates were mixed with nonreducing sodium dodecylsulfate (SDS) sample buffer supplemented with 5 mM *N*-ethylmaleimide to block unreacted thiol groups, size-fractionated by SDS polyacrylamide gel electrophoresis (PAGE) and transferred onto nitrocellulose membranes. Membranes were incubated with antibodies against NF-κB p65 (C-20), NF-κB p50 (H-119), IκBα (C-21) (all Santa Cruz Biotechnology) or GSH (ViroGen, Watertown, MA, USA). Primary antibodies were detected using horseradish peroxidase-conjugated IgG antibodies (Cell Signaling Technology, Danvers, MA, USA) and protein bands were visualised by enhanced chemiluminescence (PerkinElmer, Wellesley, MA, USA).

NF-κB/DNA binding and NF-κB p65 nuclear entry

Confluent ASMCs were serum deprived (24 h) and then pre-incubated with DMF (50 μM for 1 h) and/or GSH-OEt (1 mM for 90 min) before TNF-α stimulation (10 ng·mL^{-1} for 30 min). NF-κB/DNA binding was analysed by electrophoretic mobility shift assay (EMSA) as previously described [7]. To determine NF-κB p65 nuclear entry, cells were trypsinised and cell pellets were resuspended in low-salt buffer (10 mM 4-(2-hydroxyethyl)-1-piperazineethanesulfonic acid (HEPES), 10 mM KCl, 0.1 mM EDTA, 0.1 mM ethylene glycol tetraacetic acid (EGTA), 0.25% Nonidet P-40 and 1× protease inhibitor cocktail) for 20 min. Nuclei were incubated in high-salt buffer (20 mM HEPES, 400 mM NaCl, 1 mM EDTA, 1 mM EGTA and 1× protease inhibitor cocktail) for 40 min, size-fractionated by SDS-PAGE and transferred onto nitrocellulose membranes. The membranes were then incubated with antibodies against NF-κB p65 (C-20) or lamin A/C (Cell Signaling Technology) to confirm equal protein loading.

For immunofluorescence analysis, ASMCs were plated on cover slips and treated as described above. ASMCs were fixed with ice-cold 100% methanol (5 min at -20°C), blocked with 10% donkey serum (20 min) and incubated with an antibody against NF-κB p65 (C-20) or normal rabbit IgG for 1 h. The primary antibody was detected by addition of an Alexa488-conjugated donkey anti-rabbit IgG antibody (Invitrogen Corporation, Carlsbad, CA, USA) for 1 h. To visualise nuclei, 4,6-diamido-2-phenylindole (DAPI; Molecular Probes, Eugene, OR, USA) was added (15 min) and the cover slips were subsequently examined on a laser scanning microscope.

MAPK/MSK-1/histone H3 pathway activation

Confluent ASMCs were serum deprived for 24 h and then incubated with DMF (50 μM for 1 h) and/or GSH-OEt (1 mM for 90 min) prior to stimulation with TNF-α (10 ng·mL^{-1}) for 0, 5, 10, 15, 30, 60 or 120 min. Total cell lysates were collected, size fractionated by SDS-PAGE and transferred onto nitrocellulose membranes. Membranes were then incubated with antibodies against phospho-MSK-1 (Ser360), phospho-MSK-1 (Ser376), phospho-MSK-1 (Thr581), MSK-1, phospho-histone H3 (Ser10) (D2C8), histone H3, phospho-p38 mitogen-activated protein kinase (MAPK), p38 MAPK, phospho-extracellular signal-regulated kinase (ERK), ERK MAPK (all Cell Signaling Technology), MAPK phosphatase (MKP)-1 or α-tubulin (DM1A; Santa Cruz Biotechnology).

Chemokine secretion

Confluent ASMCs were serum deprived for 24 h, before a single drug (DMF for 1 h or GSH-OEt for 90 min), or the drugs in combination, were added prior to stimulation with TNF-α (10 ng·mL^{-1} for 24 h). Supernatants were collected, and eotaxin and RANTES were measured by ELISA (Duo Set; R&D Systems).

Data analysis

The statistical analysis was performed using Mann–Whitney U-test; p-values of $\leqslant 0.05$ were considered significant.

RESULTS

Cell characterisation

In figure 1a–i, we show that cells isolated from human bronchi expressed at least two ASMC markers (smooth muscle α-actin (α-SMA) and smooth muscle myosin heavy chain (SMMHC)), and are negative for fibronectin expression. This expression pattern of the ASMC markers is maintained until passage 10 without significant changes, and is dependent on the addition of vitamins to the cell culture medium (unpublished observations). In contrast, human bronchial myofibroblasts expressed significant levels of fibronectin, but no SMMHC and only a low level of α-SMA (fig. 1a–i).

DMF reduces ASMC GSH level

DMF reduced intracellular GSH in other cell types [14–16]. In this study, incubation of ASMC with DMF (50 μM) for 1 and 3 h reduced the level of GSH by ~50%, when compared with the vehicle-treated cells (fig. 1a–i).

Diamide induces IκBα-SSG in ASMC

It is unknown whether glutathionylation occurs in cultured ASMCs. Therefore, we first determined the effect of the well-known glutathionylation inducer diamide [11] on NF-κB/IκB. After ASMC treatment with diamide (100–500 μM for 30 min), NF-κB/IκB was immunoprecipitated with antibodies against NF-κB p65 or NF-κB p50 (fig. 1k and l). Diamide did not induce NF-κB p65-SSG or NF-κB p50-SSG (data not shown). Importantly, IκBα-SSG levels increased after diamide (500 μM) treatment when compared to untreated cells (fig. 1k and l). To confirm that the NF-κB/IκB complex was successfully co-immunoprecipitated and demonstrated equal protein loading, the membranes were incubated with antibodies against NF-κB p65, NF-κB p50 or IκBα (fig. 1b). NF-κB/IκB was not precipitated by normal rabbit IgG, demonstrating the specificity of the antibodies (fig. 1b).

DMF induces IκBα-SSG and inhibits I-κBα degradation

In order to determine whether IκBα-SSG mediates NF-κB inhibition by DMF [7], we assessed DMF effects on IκBα-SSG and IκBα degradation. NF-κB/IκB was immunoprecipitated with antibodies against NF-κB p65 or NF-κB p50 (fig. 1k and l). In unstimulated ASMCs, IκBα levels were high, but IκBα-SSG was not detectable (fig. 1m and n). In TNF-α-treated ASMCs, IκBα was fully degraded and, therefore, no IκBα-SSG was detectable (fig. 1k and l). Importantly, when DMF was added to TNF-α-stimulated ASMCs, IκBα-SSG was induced and IκBα degradation was inhibited (fig. 1m and n). In the presence of GSH-OEt, DMF did not induce IκBα-SSG (fig. 1m and n), suggesting that a reduction of ASMC GSH mediates DMF-induced IκBα-SSG. Most importantly, addition of GSH-OEt also reversed the inhibitory effect of DMF on IκBα degradation (fig. 1m and n), suggesting

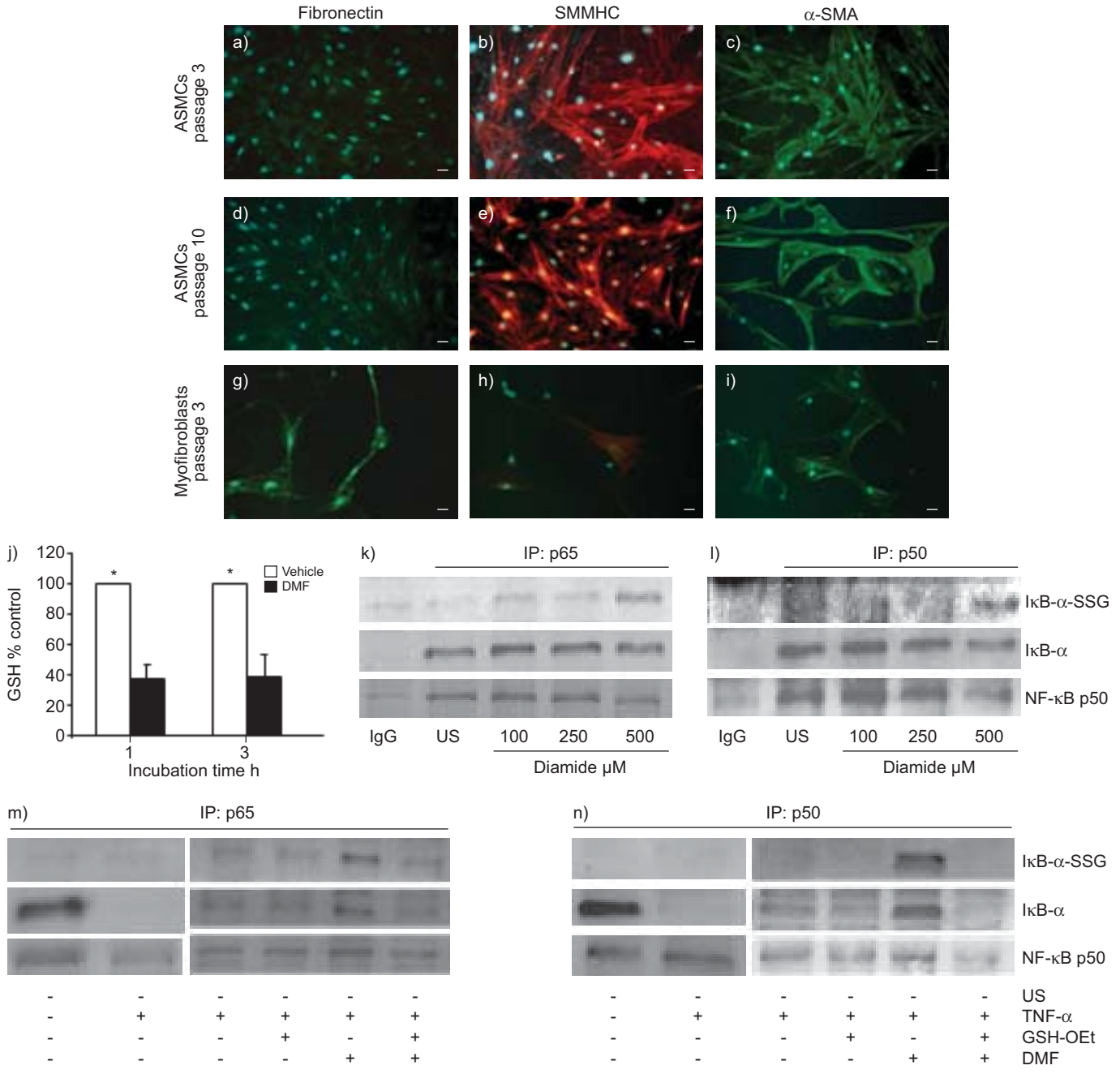

FIGURE 1. a–f) Cell characterisation for one airway smooth muscle cell (ASMC) line at passages 3 and 10. g–i) Human lung fibroblasts were used at passage 3. SMMHC: smooth muscle myosin heavy chain; α-SMA: smooth muscle α-actin. Scale bars=10 μm. j–n) Dimethylfumarate (DMF) reduces intracellular glutathione (GSH) and induces IκBα glutathionylation. j) ASMCs of three different donors were treated with DMF (50 μM) or vehicle (dimethylsulfoxide; 0.05%) and intracellular GSH was measured after 1 and 3 h. Data are presented as mean±SEM of five replicates. *: $p<0.05$ (Mann–Whitney U-test). k, l) ASMCs were treated with diamide or left unstimulated (US) for 30 min or m, n) were pre-treated with GSH ethyl ester (OEt) (1 mM for 90 min) and/or DMF (50 μM for 1 h) followed by stimulation with tumour necrosis factor (TNF)-α (10 ng·mL^{-1}) for 30 min. Cells were lysed and the nuclear factor (NF)-κB/IκB (inhibitor of NF-κB) complex was immunoprecipitated (IP) with an antibody against either NF-κB p65 or NF-κB p50 or normal rabbit immunoglobulin (Ig)G. Following immunoblotting under nonreducing conditions, the membranes were incubated with antibodies against GSH (IκBα-SSG), or total IκBα, or NF-κB p65 or p50.

that IκBα-SSG mediates the inhibition on IκBα degradation. TNF-α-induced IκBα degradation and the level of IκBα-SSG was not altered in the presence of GSH-OEt alone (fig. 1k and l). Equal protein loading was confirmed by incubating the membranes with antibodies against NF-κB p65 or NF-κB p50 (fig. 1k and l).

DMF-mediated inhibition of NF-κB is reversed by the addition of GSH-OEt

Next, we assessed whether the reversal of DMF-induced IκBα-SSG by GSH-OEt also reverses inhibition of NF-κB p65 nuclear entry and NF-κB/DNA binding by DMF [7]. Immunoblotting

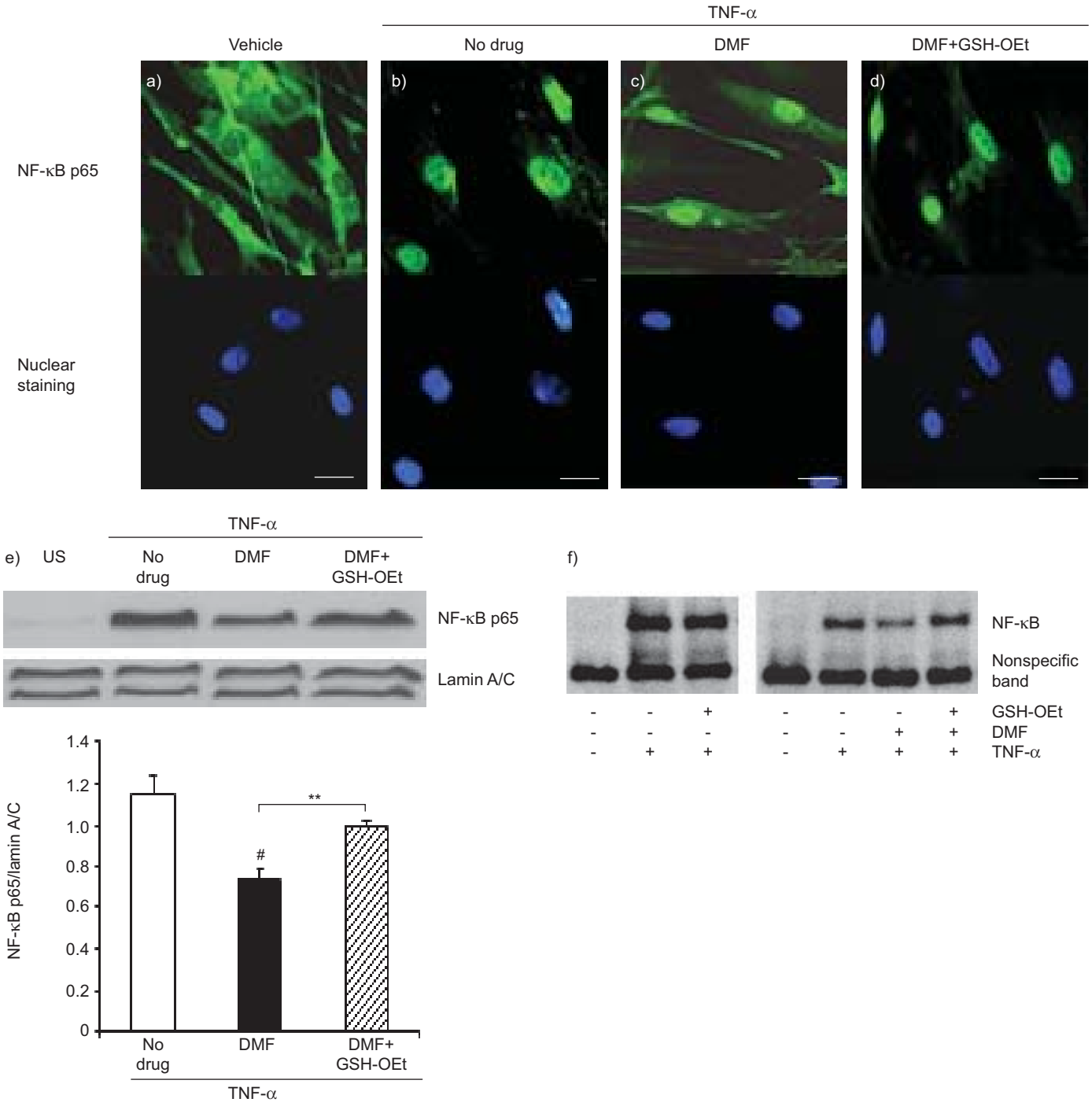

FIGURE 2. Effects of dimethylfumarate (DMF) and its reversal by glutathione (GSH) ethyl ester (OEt) on nuclear factor (NF)-κB p65 nuclear entry and NF-κB/DNA binding. a–d) Nuclear entry of NF-κB p65 is depicted by a representative fluorescence immunostaining of airway smooth muscle cells treated with GSH-OEt (1 mM for 90 min) and/or DMF (50 μM for 1 h) prior to tumour necrosis factor (TNF)-α stimulation (10 ng·mL^{-1}) for 30 min. Scale bars=10 μm. e) Nuclear entry of NF-κB p65 at 30 min after stimulation was confirmed by immunoblotting using nuclear protein extracts. The bar chart summarises the densitometric analysis of NF-κB p65 nuclear entry at 30 min, normalised to lamin A/C. Data are presented as mean±SEM of experiments performed in four different cell lines and were analysed using Mann–Whitney U-test. #: $p \leq 0.05$ for TNF-α *versus* TNF-α+DMF. **: $p<0.01$. f) Representative NF-κB-specific electrophoretic mobility shift assay. Three additional independent experiments showed comparable results.

and immunofluorescence analyses revealed that the amount of nuclear NF-κB p65 increased after stimulation with TNF-α, when compared with the vehicle control (fig. 2a–e). The TNF-α-induced NF-κB p65 nuclear accumulation (mean±SEM NF-κB p65/lamin A/C 1.15±0.09) was significantly inhibited by DMF to 0.73±0.06 ($p \leq 0.05$) (fig. 2a–e), and this inhibitory effect was reversed by the addition of GSH-OEt (fig. 2a–e). EMSA analysis showed that NF-κB/DNA binding was not detectable in unstimulated cells (fig. 2f). TNF-α induced binding of NF-κB to DNA and this was not altered by GSH-OEt (fig. 2f). Treatment

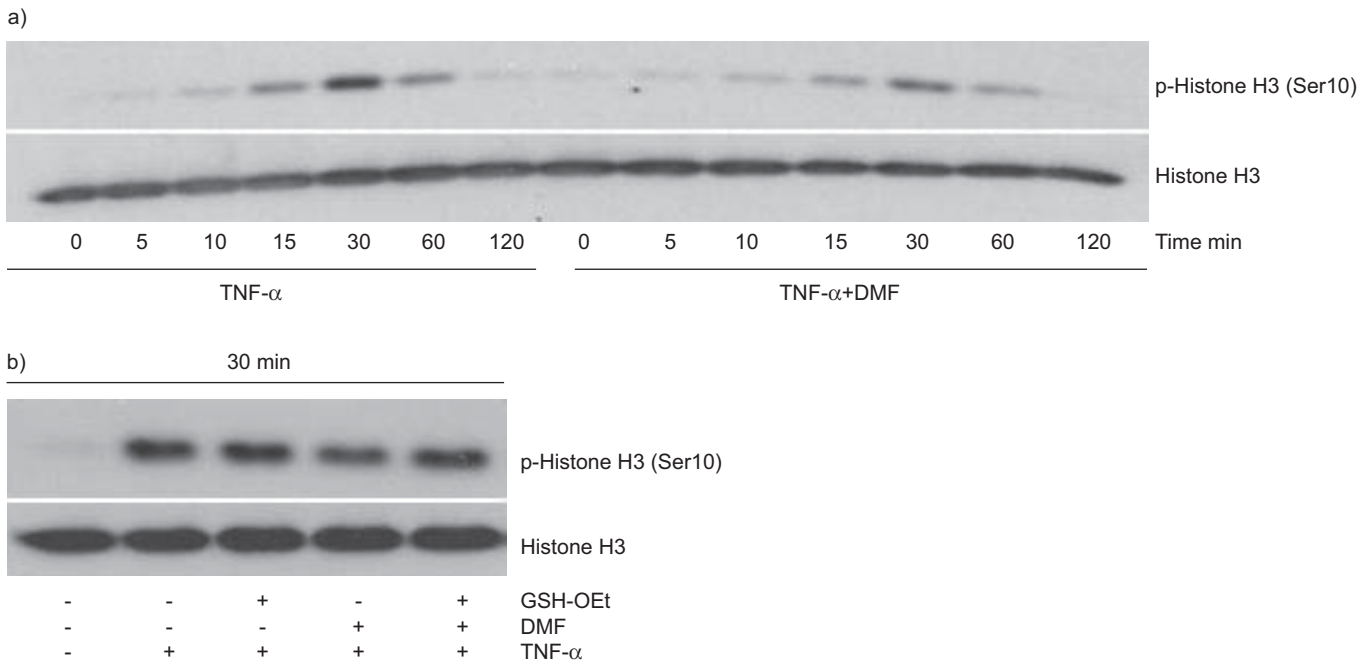

FIGURE 3. Effects of dimethylfumarate (DMF) and its reversal by glutathione (GSH) ethyl ester (OEt) on histone H3 phosphorylation (p-Histone H3). a) Airway smooth muscle cells (n=3) were treated with GSH-OEt (1mM for 90 min) and/or DMF (50 μM for 1 h) prior to stimulation with tumour necrosis factor (TNF)-α (10 ng·mL^{-1}) for the indicated times. A representative immunoblot of the kinetics of histone H3 phosphorylation at Ser10 induced by TNF-α and its inhibition by DMF is shown. b) Representative immunoblot of the reversing effect of exogenous GSH-OEt on DMF-dependent histone H3 (Ser10) inhibition at 30 min.

with DMF inhibited TNF-α-induced NF-κB/DNA binding and importantly, this was reversed by GSH-OEt (fig. 2f).

DMF inhibits histone H3 phosphorylation, which was reversed by GSH-OEt

DMF inhibited MSK-1 activity in ASMCs [7], upstream of histone H3 [20], which is important for optimal NF-κB/DNA binding [19]. Here, we show that TNF-α induces histone H3 phosphorylation between 15–60 min, with a maximal effect at 30 min, which was inhibited by DMF (fig. 3a). Since inhibition of NF-κB/DNA binding by DMF was fully reversed by addition of GSH-OEt, we were curious whether DMFs effect on histone H3 is also dependent on GSH. Interestingly, the inhibitory effect of DMF on TNF-α-induced histone H3 phosphorylation at 30 min was fully reversed by addition of GSH-OEt, whereas GSH-OEt alone had no effect on TNF-α-induced histone H3 phosphorylation (fig. 3b). TNF-α, GSH-OEt or DMF, alone or in combination, had no effect on total histone H3 protein expression (fig. 3a and b).

DMF inhibits MSK-1 independently of upstream molecules p38 and ERK MAPK

DMF inhibits MSK-1 in ASMCs [7], and this was confirmed in this study, where DMF inhibited the TNF-α-induced phosphorylation of MSK-1 at Ser376 between 10 and 30 min (fig. 4a). In contrast, TNF-α-induced phosphorylation of MSK-1 at Ser360 and Thr581 between 10 and 30 min was not affected by DMF treatment (fig. 4a). Neither TNF-α nor DMF had an effect on total MSK-1 protein expression (fig. 4a). The p38 and ERK MAPKs can phosphorylate, and thereby activate, MSK-1 [20]. Here, we show that DMF-induced MSK-1 inhibition is not mediated by an inhibition of p38 or ERK MAPK. TNF-α activated p38 MAPK phosphorylation between 5 and 30 min, which was enhanced and prolonged by DMF treatment (fig. 4b). ERK phosphorylation was induced by TNF-α between 10 and 30 min and this was not altered by DMF (fig. 4b). Total p38 and ERK MAPK protein expression was not affected by either TNF-α or DMF between 0 and 120 min (fig. 4b). TNF-α upregulated the endogenous MAPK inhibitor MKP-1 after 60 min, as previously described [23], and this was not affected by DMF (fig. 4b). Equal protein loading was confirmed by incubation of the membrane with an α-tubulin primary antibody (fig. 4b).

GSH-OEt reverses the inhibitory effect of DMF on eotaxin and RANTES

Next, we assessed whether GSH-OEt can also reverse the inhibitory effect of DMF on eotaxin and RANTES. TNF-α significantly induced eotaxin and RANTES secretion, when compared with the vehicle control, and this was inhibited by DMF (fig. 5a and b), as previously reported [7]. Importantly, the addition of GSH-OEt significantly reversed DMF's inhibitory effect on eotaxin and RANTES (fig. 5a, 5b). GSH-OEt alone had no effects on TNF-α-induced eotaxin or RANTES secretion, or the baseline levels of the two chemokines (fig. 5a and b).

DISCUSSION

In this study, we showed that IκBα-SSG and reduced histone H3 phosphorylation contribute to the inhibitory effect of DMF on NF-κB-dependent eotaxin and RANTES secretion. DMF reduced intracellular GSH in ASMCs and this has previously been shown to induce protein glutathionylation [11]. In this study, we showed for the first time that IκBα-SSG is inducible in cultured ASMCs. Furthermore, we showed that DMF inhibited the degradation of IκBα and subsequent NF-κB p65 nuclear entry, which was

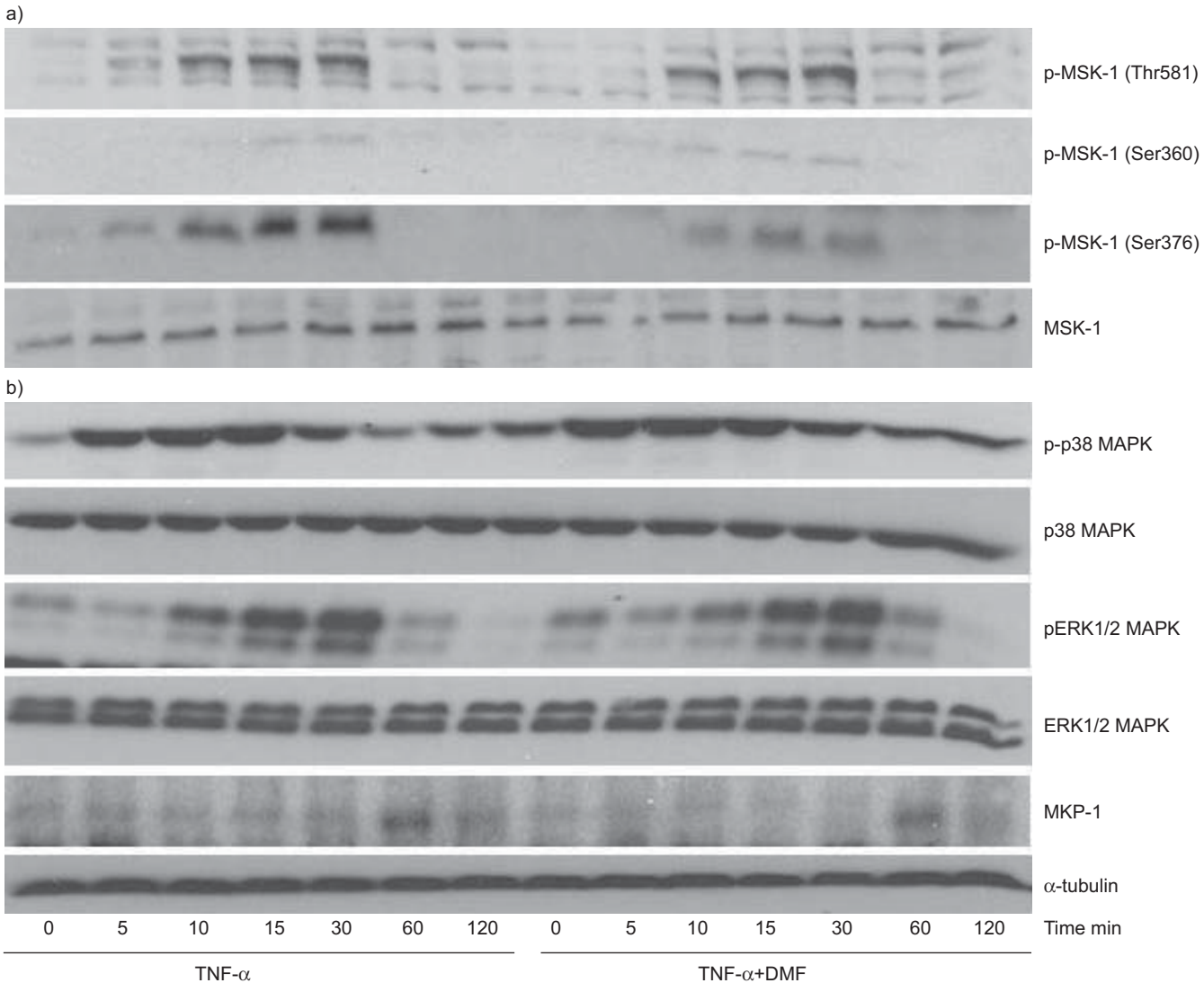

FIGURE 4. Dimethylfumarate (DMF) effects on mitogen- and stress-activated protein kinase (MSK)-1 and mitogen-activated protein kinase (MAPK) phosphorylation and on MAPK phosphatase (MKP)-1 expression. a) Airway smooth muscle cell lines (n=3) were treated with DMF 1 h prior to stimulation with tumour necrosis factor (TNF)-α for 0 to 120 min. Representative immunoblots of the kinetics of MSK-1 phosphorylation (p-MSK1) at Thr581, Ser360 and Ser376, and total MSK-1 expression. b) Representative immunoblot of p38 MAPK phosphorylation (p-p38 MAPK), total p38 MAPK expression, extracellular signal-regulated kinase (ERK)1/2 MAPK phosphorylation (p-ERK1/2 MAPK), total ERK1/2 expression, MAPK and MKP-1 expression, and the loading control α-tubulin. Similar results were obtained in two additional cell lines.

mediated by IκBα-SSG. In addition, we found that histone H3 phosphorylation, which enhances accessibility of NF-κB binding sides within promoters [19], was inhibited by DMF. This effect was most probably mediated by DMF-induced inhibition of MSK-1, which is upstream of histone H3. Importantly, not only DMF-mediated inhibition of NF-κB and histone H3 were reversed by addition of GSH-OEt, but also its inhibitory effect on eotaxin and RANTES, suggesting that DMF inhibits these factors by altering the ASMC GSH level. Taken together, our study reveals new mechanisms by which eotaxin and RANTES secretion can be inhibited in ASMCs. Development of new drugs targeting the pathways described here may help to limit eosinophilic inflammation in asthma.

NF-κB is considered to be one of the most important regulators of immune responses and was shown to play a critical role in inflammatory airways diseases [24]. NF-κB regulates the expression of many pro-inflammatory factors and its inhibition was shown to be anti-inflammatory in ASMCs [7]. Earlier studies have shown that a reduced level of intracellular GSH can inhibit NF-κB activity [25, 26]. This is in agreement with our study, which shows that DMF mediates its inhibitory effect on NF-κB *via* a reduction of intracellular GSH. Glutathionylation, which is inducible by a reduced intracellular GSH level [11], is a reversible, redox-regulated mechanism and a number of studies have shown that the NF-κB pathway was inhibited by glutathionylation on multiple levels. In tracheal epithelial cells, glutathionylation of the IκB kinase complex resulted in an inhibition of NF-κB p65 nuclear entry and NF-κB/DNA binding [27]. In HeLa cells, diamide induced the IκBα-SSG, which decreased phosphorylation and ubiquitinylation of IκBα *in vitro* [10]. Glutathionylation of the NF-κB p65 subunit was induced in cinnamaldehyde

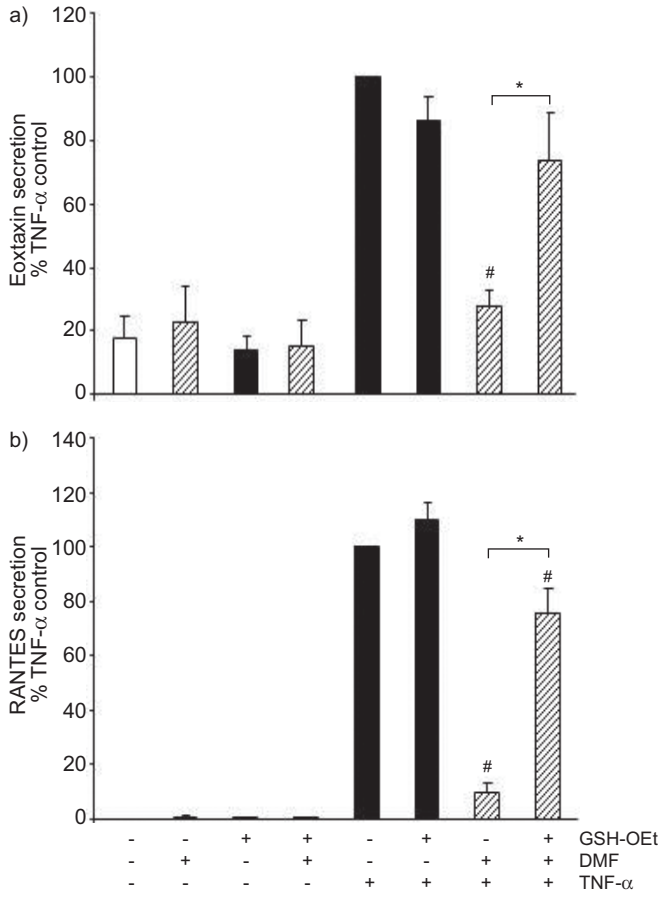

FIGURE 5. Glutathione (GSH) ethyl ester (OEt) reverses the effects of dimethylfumarate (DMF) on eotaxin and RANTES (regulated on activation, normal T-cell expressed and secreted) secretion by airway smooth muscle cells (ASMCs). ASMC lines of four different donors were treated with GSH-OEt (1 mM for 90 min) and/or DMF (50 μM for 1 h) prior to stimulation with tumour necrosis factor (TNF)-α for 24 h and a) eotaxin and b) RANTES secretion was measured by ELISA. Data are presented as mean±SEM from 6–7 replicates and were analysed using Mann–Whitney U-test. #: $p \leqslant 0.05$ for TNF-α *versus* TNF-α+drugs. *: $p<0.05$.

treated endothelial cells, leading to an inhibition of NF-κB p65 nuclear translocation [12]. *In vitro*, NF-κB p50-SSG inhibited the capacity of NF-κB to bind DNA [13]. The induction of IκBα-SSG by DMF reported here is, therefore, likely to contribute to its inhibitory effect on NF-κB nuclear entry and NF-κB/DNA binding.

Previously, it was shown that DMF inhibits the phosphorylation of MSK-1 at Ser376, resulting in reduced phosphorylation of downstream CREB (cyclic adenosine monophosphate response element binding) and NF-κB p65 [7, 21]. MSK-1 also phosphorylates histone H3 at Ser10 [20], which increases the accessibility of NF-κB binding sites within different promoters [19]. In this study, we showed that DMF inhibits the phosphorylation of histone H3, which was most probably mediated by its inhibition of MSK-1. Interestingly, the inhibitory effect of DMF on MSK-1 was not mediated by reduced activation of p38 or ERK MAPK, which is upstream of MSK-1. Furthermore, MSK-1 phosphorylation at the Ser360 and Thr581 phosphorylation sites, which are directly targeted by p38 or ERK MAPK [28], were not affected by DMF treatment. These findings are in agreement with another study in keratinocytes, showing that DMF inhibited MSK-1 phosphorylation at Ser376 independently of p38 or ERK MAPK [21]. MKP-1, an endogenous inhibitor of MAPK, can be upregulated by reduced GSH levels [29] and, besides inhibiting MAPK p38 and ERK in ASMCs [23], it was reported to dephosphorylate histone H3 at Ser10 [30]. However, DMF treatment did not affect MKP-1 level in our study, suggesting that it does not mediate the inhibitory effect of DMF on histone H3 phosphorylation. Importantly, the DMF effect on histone H3 phosphorylation was reversed by addition of GSH-OEt, suggesting that DMF-induced changes in intracellular GSH also mediate the effect of DMF on the MSK-1/histone H3 pathway. However, the exact mechanisms by which DMF inhibits the MSK-1/histone H3 pathway remains to be determined in future studies.

The DMF-dependent downregulation of eotaxin and RANTES confirmed our previous study [7], and is of particular importance, as these chemokines attract eosinophils towards the inflamed airway, which in turn alter ASMC function [1]. Earlier we found that DMF inhibits eotaxin and RANTES by inhibiting NF-κB [7]. Here, we showed that both effects were dependent on DMF-induced reduction of intracellular GSH. Similarly, DMF inhibited interleukin (IL)-1β, TNF-α and IL-6 secretion in human peripheral blood mononuclear cells, which was rescued by GSH supplementation [16]. Furthermore, DMF reduced GSH level and inhibited lipopolysaccharide-induced IL-1β, TNF-α and IL-6 secretion in glial cells [15].

In conclusion, new molecular mechanisms by which TNF-α-induced chemokine secretion can be inhibited in ASMCs have been demonstrated in this study. Targeting the pathways described here might help to reduce eosinophilic inflammation in asthma.

SUPPORT STATEMENT

This study was supported by a grant from a Swiss National Foundation grant (320030-116022) and by a grant of the Gottfried and Julia Bangerter–Rhyner Stiftung (Berne, Switzerland).

STATEMENT OF INTEREST

None declared.

REFERENCES

1 Kay AB. The role of eosinophils in the pathogenesis of asthma. *Trends Mol Med* 2005; 11: 148–152.
2 Ying S, Meng Q, Zeibecoglou K, *et al*. Eosinophil chemotactic chemokines (eotaxin, eotaxin-2, RANTES, monocyte chemoattractant protein-3 (MCP-3), and MCP-4), and C-C chemokine receptor 3 expression in bronchial biopsies from atopic and nonatopic (intrinsic) asthmatics. *J Immunol* 1999; 163: 6321–6329.
3 Berkman N, Krishnan VL, Gilbey T, *et al*. Expression of RANTES mRNA and protein in airways of patients with mild asthma. *Am J Respir Crit Care Med* 1996; 154: 1804–1811.
4 Li D, Wang D, Griffiths-Johnson DA, *et al*. Eotaxin protein and gene expression in guinea-pig lungs: constitutive expression and upregulation after allergen challenge. *Eur Respir J* 1997; 10: 1946–1954.
5 Thomas PS, Yates DH, Barnes PJ. Tumour necrosis factor-α increases airway responsiveness and sputum neutrophilia in normal human subjects. *Am J Respir Crit Care Med* 1995; 152: 76–80.

6 Brightling CE, Bradding P, Symon FA, *et al.* Mast-cell infiltration of airway smooth muscle in asthma. *N Engl J Med* 2002; 346: 1699–1705.
7 Seidel P, Merfort I, Hughes JM, *et al.* Dimethylfumarate inhibits NF-κB function at multiple levels to limit airway smooth muscle cell cytokine secretion. *Am J Physiol Lung Cell Mol Physiol* 2009; 297: L326–L339.
8 Nie M, Knox AJ, Pang LH. β-2-adrenoceptor agonists, like glucocorticoids, repress eotaxin gene transcription by selective inhibition of histone H4 acetylation. *J Immunol* 2005; 175: 478–486.
9 Chen LF, Greene WC. Shaping the nuclear action of NF-κB. *Nat Rev Mol Cell Biol* 2004; 5: 392–401.
10 Kil IS, Kim SY, Park JW. Glutathionylation regulates IκB. *Biochem Biophys Res Commun 2008; 15*, 373: 169–173.
11 Gilge JL, Fisher M, Chai YC. The effect of oxidant and the non-oxidant alteration of cellular thiol concentration on the formation of protein mixed-disulfides in HEK 293 cells. *PLoS One* 2008; 3: e4015.
12 Liao BC, Hsieh CW, Lin YC, *et al.* The glutaredoxin/glutathione system modulates NF-κB activity by glutathionylation of p65 in cinnamaldehyde-treated endothelial cells. *Toxicol Sci* 2010; 116: 151–163.
13 Pineda-Molina E, Klatt P, Vázquez J, *et al.* Glutathionylation of the p50 subunit of NF-κB: a mechanism for redox-induced inhibition of DNA binding. *Biochemistry* 2001; 40: 14134–14142.
14 Thiessen A, Schmidt MM, Dringen R. Fumaric acid dialkyl esters deprive cultured rat oligodendroglial cells of glutathione and upregulate the expression of heme oxygenase 1. *Neurosci Lett* 2010; 475: 56–60.
15 Wierinckx A, Brevé J, Mercier D, *et al.* Detoxication enzyme inducers modify cytokine production in rat mixed glial cells. *J Neuroimmunol* 2005; 166: 132–143.
16 Lehmann JC, Listopad JJ, Rentzsch CU, *et al.* Dimethylfumarate induces immunosuppression *via* glutathione depletion and subsequent induction of heme oxygenase 1. *J Invest Dermatol* 2007; 127: 835–845.
17 Kouzarides T. Chromatin modifications and their function. *Cell* 2007; 128: 693–705.
18 Ahn YT, Huang B, McPherson L, *et al.* Dynamic interplay of transcriptional machinery and chromatin regulates ''late'' expression of the chemokine RANTES in T lymphocytes. *Mol Cell Biol* 2007; 27: 253–266.
19 Saccani S, Pantano S, Natoli G. p38-dependent marking of inflammatory genes for increased NF-κB recruitment. *Nat Immunol* 2002; 3: 69–75.
20 Vermeulen L, Berghe WV, Beck IM, *et al.* The versatile role of MSKs in transcriptional regulation. *Trends Biochem Sci* 2009; 34: 311–318.
21 Gesser B, Johansen C, Rasmussen MK, *et al.* Dimethylfumarate specifically inhibits the mitogen and stress-activated kinases 1 and 2 (MSK1/2): possible role for its anti-psoriatic effect. *J Invest Dermatol* 2007; 127: 2129–2137.
22 Johnson PRA, Roth M, Tamm M, *et al.* Airway smooth muscle cell proliferation is increased in asthma. *Am J Respir Crit Care Med* 2001; 164: 474–477.
23 Quante T, Ng YC, Ramsay EE, *et al.* Corticosteroids reduce IL-6 in ASM cells *via* up-regulation of MKP-1. *Am J Respir Cell Mol Biol* 2008; 39: 208–217.
24 Janssen-Heininger YM, Poynter ME, Aesif SW, *et al.* Nuclear factor κB, airway epithelium, and asthma: avenues for redox control. *Proc Am Thorac Soc* 2009; 6: 249–255.
25 Mihm S, Galter D, Dröge W. Modulation of transcription factor NFκB activity by intracellular glutathione levels and by variations of the extracellular cysteine supply. *FASEB J* 1995; 9: 246–252.
26 Lou H, Kaplowitz N. Glutathione depletion down-regulates tumour necrosis factor α-induced NF-κB activity *via* IκB kinase-dependent and -independent mechanisms. *J Biol Chem* 2007; 282: 29470–29481.
27 Reynaert NL, van der Vliet A, Guala AS, *et al.* Dynamic redox control of NF-κB through glutaredoxin-regulated *S*-glutathionylation of inhibitory κB kinase β. *Proc Natl Acad Sci USA* 2006; 103: 13086–13091.
28 McCoy CE, Campbell DG, Deak M, *et al.* MSK1 activity is controlled by multiple phosphorylation sites. *Biochem J* 2005; 387: 507–517.
29 Kim SM, Park JG, Baek WK, *et al.* Cadmium specifically induces MKP-1 expression *via* the glutathione depletion-mediated p38 MAPK activation in C6 glioma cells. *Neurosci Lett* 2008; 440: 289–293.
30 Kinney CM, Chandrasekharan UM, Yang L, *et al.* Histone H3 as a novel substrate for MAP kinase phosphatase-1. *Am J Physiol Cell Physiol* 2009; 296: C242–C249.